INTERNATIONAL JOURNAL OF ENERGY RESEARCH
Int. J. Energy Res. (2008)
Published online in Wiley InterScience
(www.interscience.wiley.com). DOI: 10.1002/er.1419

Microbial fuel cells based on carbon veil electrodes: Stack configuration and scalability

Ioannis Ieropoulos[1,*,†], John Greenman[2] and Chris Melhuish[1]

[1]*Bristol Robotics Laboratory, Bristol Business Park, Coldharbour Lane, Universities of Bristol and of the West of England, Bristol Business Park, Coldharbour Lane, BS16 1QY, U.K.*
[2]*Microbiology Research Lab, Applied Sciences Faculty, University of the West of England, Frenchay Campus, Coldharbour Lane, BS16 1QY, U.K.*

SUMMARY

The aim of this study was to compare the performance of three different sizes of microbial fuel cell (MFC) when operated under continuous flow conditions using acetate as the fuel substrate and show how small-scale multiple units may be best configured to optimize power output. Polarization curve experiments were carried out for individual MFCs of each size, and also for stacks of multiple small-scale MFCs, in series, parallel and series–parallel configurations. Of the three combinations, the series–parallel proved to be the more efficient one, stepping up both the voltage and current of the system, collectively. Optimum resistor loads determined for each MFC size during the polarization experiments were then used to determine the long-term mean power output. In terms of power density expressed as per unit of electrode surface area and as per unit of anode volume, the small-sized MFC was superior to both the medium- and large-scale MFCs by a factor of 1.5 and 3.5, respectively. Based on measured power output from 10 small units, a theoretical projection for 80 small units (giving the same equivalent anodic volume as one large 500 mL unit) gave a projected output of 10 W m^{-3}, which is approximately 50 times higher than the recorded output produced by the large MFC. The results from this study suggest that MFC scale-up may be better achieved by connecting multiple small-sized units together rather than increasing the size of an individual unit. Copyright © 2008 John Wiley & Sons, Ltd.

KEY WORDS: microbial fuel cells; scalability; stack configuration; maximum power transfer; internal resistance; fluidic conductance; continuous flow; mixed culture

1. INTRODUCTION

The earliest report regarding microbial fuel cells (MFCs) [1] was the first description of an interesting biological phenomenon: the ability of microorganisms to transform organic substrates (chemical energy) into electricity. However, these systems remained merely a scientific curiosity due to their extremely low power outputs. In recent times, improvements in MFC energy production combined with the emergence of low power electronic modules and actuators has permitted the employment of

*Correspondence to: Ioannis Ieropoulos, BRL, Bristol Business Park, Coldharbour Lane, Bristol, BS16 1QD, U.K.
†E-mail: Ioannis.ieropoulos@brl.ac.uk, URL: http://www.brl.ac.uk

Contract/grant sponsor: Engineering and Physical Sciences Research Council (EPSRC, U.K.)

Received 12 October 2007
Revised 25 February 2008
Accepted 28 February 2008

Copyright © 2008 John Wiley & Sons, Ltd.

MFCs in real applications as exemplified by Gastrobot [2] and EcoBots-I and -II [3,4].

In the early stages of MFC development, artificial mediators were widely used [5–7], (reviewed by Palmore and Whitesides [8]) in the anodic chamber. These are becoming obsolete since the discovery that some species of microbes can produce electroactive metabolites (e.g. sulphide), which act as natural mediators [9]. In conjunction with this, complex mixed species consortia were reported to outperform any monoculture-based MFCs in terms of power output [9–13] and at the same time widen the range of utilizable organic substrates [4,14,15]. Moreover, the discovery of anodophiles (or electrophiles) such as *Geobacter* or *Rhodoferrax* species [16,17] that conduct electrons directly to the anode by physical contact has further marginalized the use of artificial mediators. The majority of MFC experiments reported in the literature are batch culture systems with the disadvantage of discontinuity; the relatively recent development of continuous flow MFCs [10,18–21] has enabled longer-term performances to be realized.

Developments have also been reported for the cathodic systems, moving from those based on chemical electrolytes (e.g. ferricyanide) as the terminal electron sink (oxidizer) [8,22] to ones based on oxygen electrodes, which offer the advantage of self sustainability, provided they are kept hydrated in oxygenated environments [14,23–25].

The key advantage of MFCs over other types of small-scale energy sources (e.g. batteries) is that their construction, fuel sources and operation are environmentally friendly. The cost of manufacture is low and the production of electricity has the potential of being continuous over months or years, as long as there is continuous or periodic replenishment of nutrients. MFCs possess high substrate to electricity conversion efficiencies (up to 96%) [16], but their primary disadvantage is the low energy transformation rates, which currently limits this technology to only low power applications. These could conceivably include sensors, indicator lights, electronic processors, small actuators and small robots. The typical sustainable voltage output from a 25-mL-sized MFC with a ferricyanide cathode and carbon veil electrodes is of the order of 0.7 V (open circuit). Higher open-circuit values of ~ 1 V have also been reported from individual small-scale MFCs under special conditions [26,27], which are closer to the theoretical maximum of 1.14 V. Thus, in order to produce sufficient voltage (>1.5 V) and/or power—to reside within the operating range of silicon-based circuitry—it is necessary to either scale-up one single unit or connect multiple small units together.

For conventional (chemical) fuel cells—as with conventional batteries—it is well known that a large number of units connected together will produce more power than a single unit [28]. The same applies to MFCs, as shown by EcoBots-I and -II, which employed stacks of 8 MFCs connected together [3,4] and also more recently demonstrated in a continuous flow stack of 6 units [29]. However, it is still unknown whether increasing the volume of a single MFC unit (for example) 20-fold has any advantage over joining 20 single small units together (with equivalent total anodic volume). A further issue is encountered when connecting multiple units together, as this can be done in a number of different ways, in series, parallel or series/parallel (see Figure 1), to step-up the voltage, current or both, respectively. The connection of multiple MFCs may be further complicated if the units are running under continuous flow conditions, which involves electrically conducting fluidic connections.

This study builds on our previous work with the medium-sized MFC. This model was extensively investigated in order to determine the optimum electrode size-to-fluid volume ratio and also the optimum proton-exchange-membrane (PEM) window size, taking into consideration both intuitive and non-intuitive factors such as electrode and electrolyte resistance, electrode compaction and fluid displacement [15].

In this paper, we describe a set of experiments using MFCs of different sizes (termed as large, medium and small), which are compared by means of polarization runs and also at optimum external resistor loads and we investigate the

Copyright © 2008 John Wiley & Sons, Ltd.

DOI: 10.1002/er

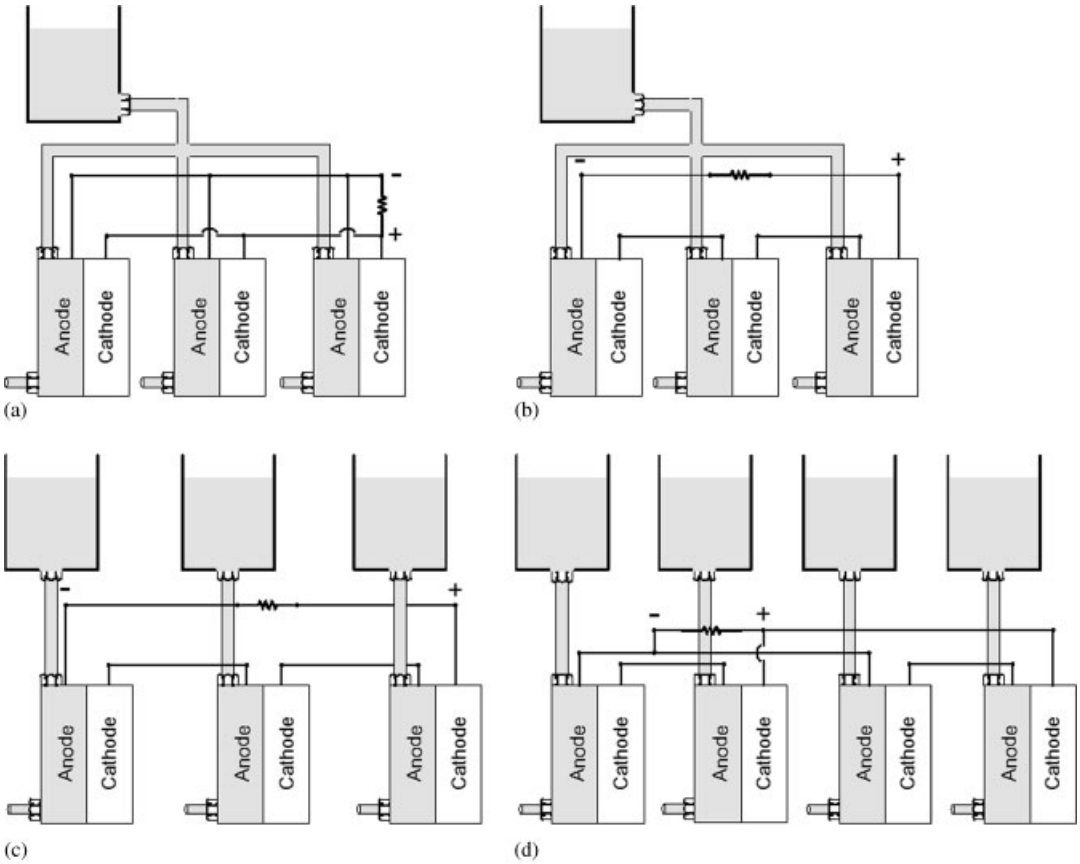

Figure 1. Schematic representation of the different fluidic and electrical configurations for stacks of MFCs: (a) parallel electrical connection with a common feed line; (b) series electrical connection with a common feed line; (c) series electrical connection but with individual feed lines; and (d) series–parallel connections with individual feed lines and with an even number of MFCs.

connection of multiple small-sized MFC units in a conventional series, parallel or series–parallel configuration, under a continuous flow mode. The overall aim is to propose an optimum configuration for scaling-up MFCs as stacks of multiple units to energize practical small-scale applications.

2. EXPERIMENTAL SETUP

2.1. Anaerobic sludge

Anaerobic-activated sewage sludge was provided by the Wessex Water Scientific Laboratory, Saltford, U.K. The collected samples were pre-processed, during treatment at the water works in order to remove pathogenic viruses. Samples were kept in their original water-based suspension, at 4°C anaerobically, and used within 3 weeks following anaerobic treatment. The sludge samples (pH 7.3) were mixed with sterile nutrient broth ($25\,g\,l^{-1}$) (Oxoid, Basingstoke, U.K.) and given 24 h at room temperature prior to usage as start inocula in the experiments.

2.2. MFC design and operation

Three MFC sizes were employed for the experiments: small, medium and large with anodic

Copyright © 2008 John Wiley & Sons, Ltd.

DOI: 10.1002/er

void volumes of 6.3, 29.63 and 652.5 mL. The medium-sized MFC has been previously used in our work and formed the control for the experiments. In terms of proportionality, the small MFC was 1/4 and the large was 20 times the size of the control. The internal dimensions ($h \times w \times d$) in mm for the three sizes were $28.5 \times 17.0 \times 3.0$ (small), $53.0 \times 43.0 \times 13.0$ (medium) and $145 \times 90 \times 50$ (large). The fluid volumes in each of the compartments were sufficient to fully cover the electrode material.

The electrode material used was pure carbon fibre veil (without catalytic metals), with a density of $20\,g\,m^{-2}$ (PRF Composites, Dorset, U.K.). The electrode surface area (s.a.) for the control (medium-sized) MFC was previously determined in a volume-to-s.a. ratio optimization experiment and was found to be $270\,cm^2$ [15]. Thus, the electrode s.a. for the small- and large-sized MFCs were proportional to the volume scale difference with the control, i.e. $67.5\,cm^2$ ($270\,cm^2/4$) for the small and $5400\,cm^2$ ($270\,cm^2 \times 20$) for the large-sized MFCs. These electrode materials were employed for both anodes and cathodes and were folded down to ($h \times w \times d$) mm: small ($15 \times 15 \times 5$), medium ($40 \times 20 \times 10$) and large ($140 \times 50 \times 50$).

Each MFC consisted of a single chamber (anode) with one open side that was sealed with the PEM (VWR, Leicestershire, U.K.), on which the O_2 cathode electrode resided thus exposing it to oxygen in air. The O_2 electrodes were frequently hydrated, to ensure full saturation with water throughout the experiments. All three systems were designed to allow continuous feed of 5 mM sodium acetate as the fuel. The membrane window size was 4.8, 18 and $36\,cm^2$ for the small-, medium- and large-sized MFCs. The PEM size was proportional to the fuel cell size decrement for the small MFC (i.e. 1/4 of the medium MFC size PEM window) but disproportional to the fuel cell size increment for the large MFC (i.e. $2\times$ larger instead of $20\times$). This was due to the physical dimensions and geometrical limitations of the large MFC available. The medium- and large-sized MFCs were assembled using 5 mm nylon studding, washers and nuts, whereas the small-sized MFC was an in-house rapid-prototyped plug-in assembly made from polycarbonate material (FDM Titan, LaserLine, Bedford, U.K.).

2.3. Polarization curve method

Polarization curves were generated using continuous flow of feedstock into the MFCs at constant flow rates to give anodic chamber dilution rates of $0.04\,h^{-1}$. Polarization data were produced by sweeping 57 resistor values covering the range of 1–29999 Ω and the time interval between resistance changes was 30 s.

2.4. Data capture

Electrode output was recorded in millivolts (mV) against time by using an ADC-16 A-D converter computer interface (Pico Technology Ltd., Cambridgeshire, U.K.). Recorded data were processed and analysed using the GraphPad Prism® version 4 software package (GraphPad, San Diego, California, U.S.A.).

2.5. Calculation of power output

The current, I, in amperes (A) was calculated using Ohm's law, $I = V/R$, where V is the measured voltage in volts (V) and R is the known value of the external load resistor in ohms (Ω). Power (P) in watts (W) of the MFCs was therefore calculated by multiplying voltage with current, i.e. $P = I \times V$. Power density in terms of electrode s.a. was calculated by $P_{\mathrm{Density}} = P/\alpha$, where α is the electrode s.a. in square-meters (m^2) and in terms of anodic chamber volume by $P_{\mathrm{Density}} = P/\mathrm{Vol}_{\mathrm{Anode}}$ where $\mathrm{Vol}_{\mathrm{Anode}}$ is the anodic fluid volume in m^3.

2.6. Internal resistance (R_{INT})

The internal resistance (R_{INT}) of any power source can be determined by applying Kirchoff's voltage law to a circuit where a voltage source is connected to a known load. This principle is ubiquitous in the field of physics, as it takes into consideration all internal losses.

For all polarization experiments, R_{INT} was determined by first recording the steady-state open-circuit voltage and then by measuring the

Copyright © 2008 John Wiley & Sons, Ltd.

DOI: 10.1002/er

steady-state current output after a resistive load (known value) was connected, for each of the different scale MFCs. R_{INT} was therefore determined by

$$R_{INT} = \left(\frac{V_{O-C}}{I_L}\right) - R_L \quad (1)$$

V_{o-c} is the open circuit of the MFC, I_L is the current under a load and R_L is the value of the load resistor.

2.7. Maximum power transfer versus maximum efficiency η

The maximum power transfer (MPT) theorem (also known as Jacobi's law) can be defined as the maximum level of power that a source with a fixed R_{INT} can deliver across a load and it is not synonymous with maximum efficiency. MPT is actually the equivalent of 50% efficiency and is achieved when $R_L = R_{INT}$ (impedance matching), which occurs when $V_L = \frac{1}{2}V_{O-C}$. Maximum efficiency, on the other hand, is achieved as $R_L \rightarrow \infty$, as less power is dissipated as heat across the external load and finally efficiency $\eta \rightarrow 0\%$ as $R_L \rightarrow 0\,\Omega$.

3. RESULTS AND DISCUSSION

3.1. Polarization curves for small, medium and large MFC in continuous flow

The data presented in Figure 2 show the power curve for each type of MFC.

For the small-scale MFC MPT was achieved at $\frac{1}{2}V_{O-C}$ reaching $0.41\,mW\,m^{-2}$ ($0.44\,W\,m^{-3}$) with a corresponding current density of $3\,mA\,m^{-2}$ ($3.24\,A\,m^{-3}$). The cell open-circuit voltage was in line with the other MFC sizes (i.e. $\sim 440\,mV$). From the voltage curve (see Figure 3), it was shown that ohmic losses were dominant.

The power density (P_D) produced from the medium-sized MFC at $\frac{1}{2}V_{O-C}$ was $0.35\,mW\,m^{-2}$ ($0.378\,W\,m^{-3}$) with a corresponding I_D of $2.7\,mA\,m^{-2}$ ($2.3\,A\,m^{-3}$). The maximum power (peak P_D) was $0.44\,mW\,m^{-2}$ and current (peak I_D) ($5\,mA\,m^{-2}$) were produced at a lower than $\frac{1}{2}V_{O-C}$ cell potential (125 mV). The open-circuit voltage from this MFC was $\sim 440\,mV$. Compared with the small MFC, P_D produced from the medium-sized MFC at $\frac{1}{2}V_{O-C}$ was 1.2-fold lower, whereas the maximum P_D was similar. The voltage curve (Figure 3) suggests that activation losses

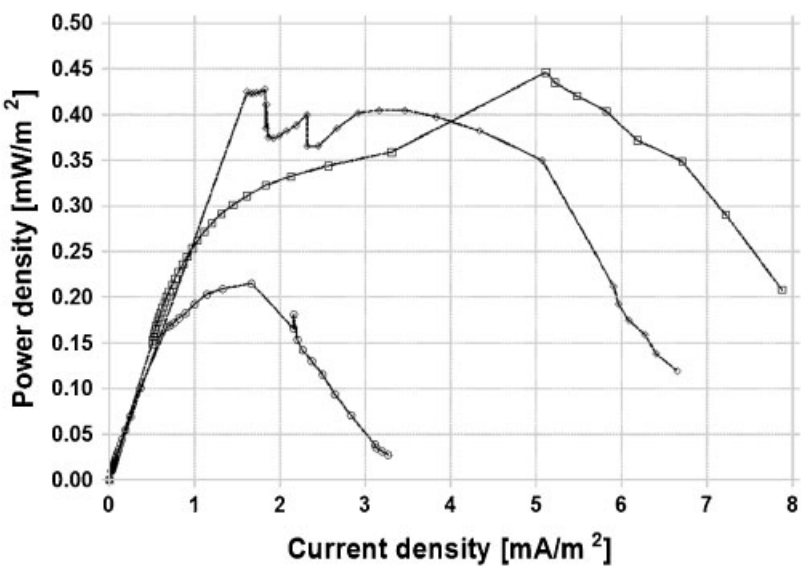

Figure 2. Power curves for the three MFC sizes. The small-scale MFC data are represented by (◇), medium-scale by (□) and large-scale by (○).

Copyright © 2008 John Wiley & Sons, Ltd.

DOI: 10.1002/er

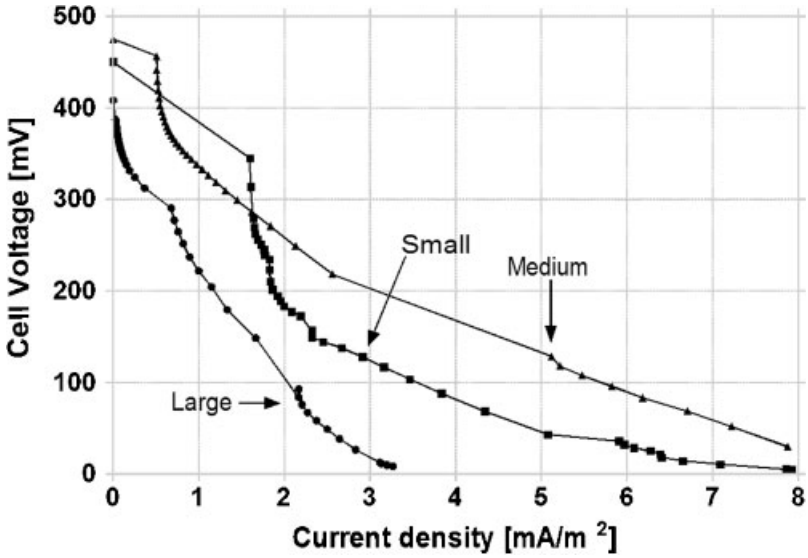

Figure 3. Polarization data for the three MFC sizes. The small-scale MFC data are represented by (■), medium-scale by (▲) and large-scale by (●).

were prevailing for I_D values from $0 \rightarrow 3.5\,mA\,m^{-2}$, whereas ohmic losses were dominating the rest of the I_D spectrum.

The maximum P_D produced from the large-scale MFC was $0.21\,mW\,m^{-2}$ ($0.226\,W\,m^{-3}$). The corresponding I_D was $1.7\,mA\,m^{-2}$ ($1.83\,A\,m^{-3}$). These values were almost half the peak P_D values produced from the small- and medium-sized MFCs. The open-circuit voltage was in line with the smaller-sized MFCs ($\sim 450\,mV$). As can be seen from the large cell voltage curve (Figure 3), for most of the I_D spectrum, ohmic losses were predominant and only minimal levels of activation losses were recorded at low I_D values. Notably, there were no mass transfer losses recorded.

$V_{O\text{-}C}$ from the individual MFCs was of the order of $\sim 450\,mV$, which is consistent for MFCs using plain unmodified carbon fibre veil electrodes. This $V_{O\text{-}C}$ value was lower than the values typically reported for MFCs using exotic metal catalysts in the cathodes or for those using flowing oxygenated water as the catholyte [27] where open-circuit voltages of the order of 1 V have been achieved.

3.2. Polarization data for multiple small MFCs connected in series, parallel and series/parallel configurations

Figure 4 shows the polarization data from 10 identical small-scale MFCs connected in series, parallel and series/parallel configurations. The latter was achieved by connecting pairs of MFCs in series and the 5 pairs in parallel. All three sets of experiments were conducted in continuous flow in which the 10 MFC units were fed from a common source bottle.

The peak P_D from the 10 MFCs connected in series was $0.42\,mW\,m^{-2}$ ($0.45\,W\,m^{-3}$) with a corresponding I_D of $0.67\,mA\,m^{-2}$ ($0.72\,A\,m^{-3}$). Compared with the single small-scale MFC, $V_{O\text{-}C}$ recorded from this experiment was approximately 1400 mV (3.2-fold higher). This value was below the predicted theoretical figure, which (for 10 units in series) would be expected to be 4400 mV ($10 \times 440\,mV$). In terms of P_D, the level produced from this stack was marginally higher than that produced from the single small-scale MFC. The cell voltage curve (Figure 5) suggests that the stack of 10 MFCs in series was mainly limited by ohmic losses.

Copyright © 2008 John Wiley & Sons, Ltd.

DOI: 10.1002/er

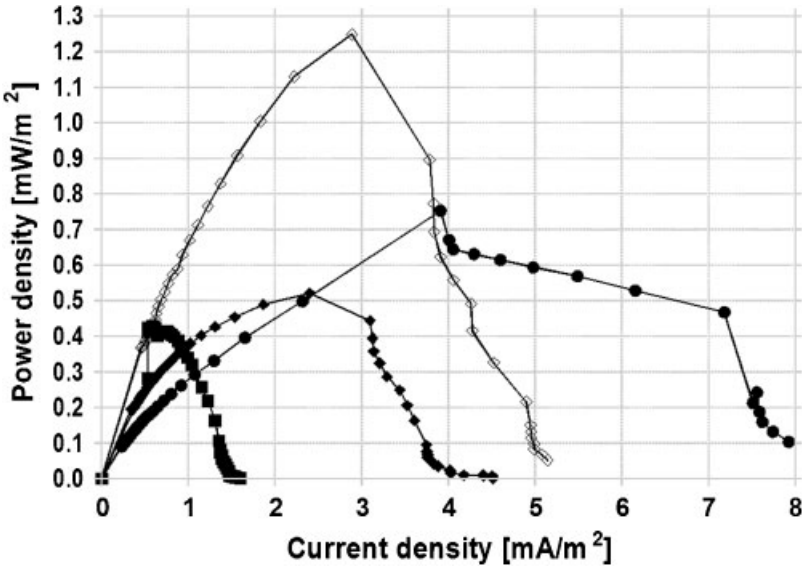

Figure 4. Power curves for the four multiple MFC configurations. Symbols show series connection (■), parallel connection (●), series–parallel (♦) and series–parallel, fluidically isolated (◇).

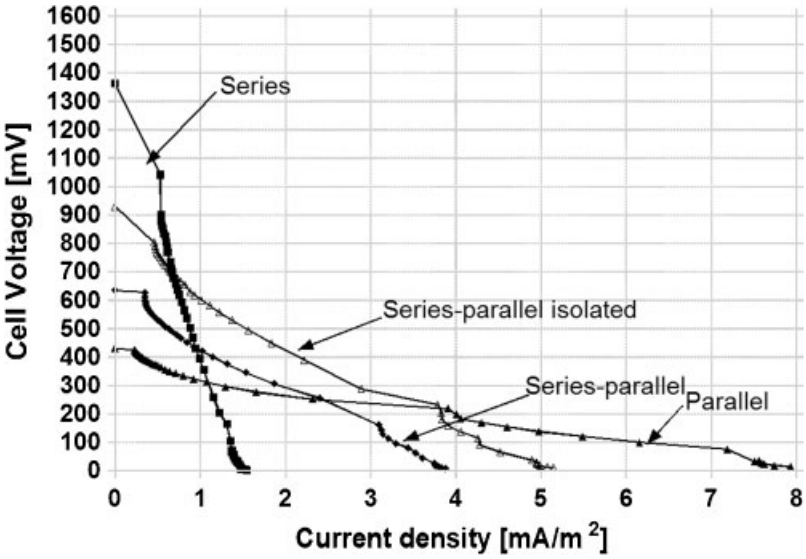

Figure 5. Polarization data for multiple MFC configurations of 10 small units. Symbols show series-connected (■), series–parallel (♦) and parallel-connected MFCs (▲). The open symbols show the series–parallel configuration with fluidically isolated units.

When the 10 MFCs were connected in parallel (Figure 4), the peak P_D produced was $0.75\,mW\,m^{-2}$ ($0.81\,W\,m^{-3}$). The corresponding I_D was $3.9\,mA\,m^{-2}$ ($4.2\,A\,m^{-3}$). Compared with the single small-scale MFC the $V_{O\text{-}C}$ value was identical ($\sim 440\,mV$), P_D was 1.8-fold higher and I_D was 1.3-fold higher. Compared with the single medium-sized MFC $V_{O\text{-}C}$ was again identical, and

Copyright © 2008 John Wiley & Sons, Ltd.

DOI: 10.1002/er

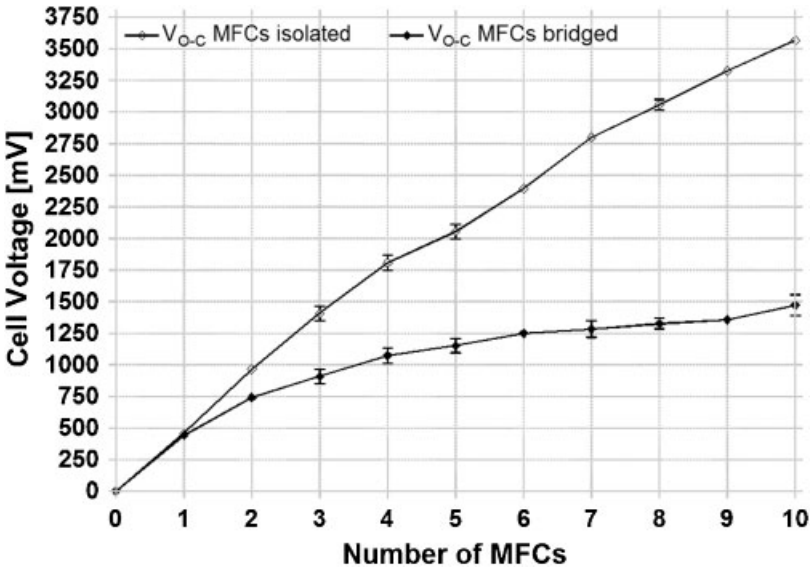

Figure 6. $V_{O\text{-}C}$ for increasing number of MFCs connected in series, when the units were bridged (fed from the same bottle) or isolated (fed with individual lines). Error bars indicate maxima and minima for $n = 3$.

P_D produced from the stack was 1.8-fold higher. P_D and I_D produced from the stack were 3.6-fold and 2.3-fold higher when compared with the single large-sized MFC. The stack voltage curve (Figure 5) suggests that although the main losses covering the wider I_D range were ohmic, the stack also suffered from low levels of activation losses.

For the series/parallel configuration (Figures 4,5), $V_{O\text{-}C}$ was ~ 700 mV, which was lower than the expected 880 mV (2×440 mV). The peak P_D (Figure 4) was 0.52 mW m^{-2} (0.56 W m^{-3}), but occurred at a cell voltage of 250 mV rather than at $\frac{1}{2}V_{O-C}$ and was 5% higher than P_D [0.49 mW m^{-2} (0.53 W m^{-3})] measured at $\frac{1}{2}V_{O-C}$. The peak P_D was 1.27-fold, 1.1-fold and 2.4-fold higher compared with the values derived from the single small-, medium- and large-sized MFCs, respectively. When compared against the alternative stack configurations, P_D from this stack was 1.2-fold higher than that produced from the purely in series and approximately 30% of the value derived from the purely in parallel configurations.

When the same 10 small MFCs were connected in the same series/parallel configuration, but fed from individual lines, i.e. fluidically isolated (Figure 4, open symbols), P_D produced was 2.5-fold higher than that recorded from the same configuration in which the MFCs were fluidically bridged (Figure 4 closed rhombus symbols). V_{O-C} was ~ 900 mV, which is in line with the theoretical 2×440 mV. P_D at $\frac{1}{2}V_{O-C}$ was 1.15 mW m^{-2} (1.24 W m^{-3}) with a corresponding I_D of 2.3 mA m^{-2} (2.48 A m^{-3}). The peak P_D produced was slightly higher at 1.25 mW m^{-2} (1.35 W$-$m^{-3}) at an I_D of 2.9 mA m^{-2} (3.13 A m^{-3}). When compared against the single small-scale MFC, this stack produced a P_D that was 2.74-fold higher.

Figure 6 illustrates the $V_{O\text{-}C}$ output from two stacks in which the MFCs were successively connected in series. In one stack, the units were fluidically bridged, whereas in the other they were fluidically isolated.

As can be seen from these data, $V_{O\text{-}C}$ from the fluidically isolated configuration was in general higher than that produced from the fluidically bridged arrangement, which appeared to be suffering from shunt losses. The output from the isolated units was 1.3-fold, 1.8-fold and 2.4-fold higher for 2, 5 and 10 units, respectively, than that produced from the fluidically bridged units. However, it was also noted that even in the case

Copyright © 2008 John Wiley & Sons, Ltd.

DOI: 10.1002/er

of the isolated units, the stack voltage produced from 6 or more MFCs connected together was lower than the anticipated theoretical value. For example, for 10 MFCs the stack voltage was 3600 mV rather than the theoretical 4400 mV.

4. GENERAL DISCUSSION

It is widely known that in conventional chemical fuel cells, electrochemical impedance spectroscopy (EIS) and current interrupt methods are standard practice, and it is now almost becoming standard practice in microbial fuel cell work as well. Yet, the length of time used to record the data points for calculating the internal resistance is often insufficient, as this does not allow for true steady states to be reached, which for an MFC can be up to several minutes rather than a few milliseconds, which is typical for conventional chemical fuel cells. During this very short period of time, the MFC is still in transition settling from its open circuit (or loaded) to its loaded (or open circuit) state, and therefore its internal resistance is varying. The internal resistance of the medium-sized MFC measured by EIS using a potentiostat with a frequency response analyser module (Versastat[3]-400 with FRA, results not shown) was found to be 12 Ω compared with the R_{INT} value of 1.3 kΩ already calculated using Equation (1). If the R_{INT} value was really only 12 Ω, then the predicted current output from the medium-sized MFC should have been approximately 20 mA, a figure of 2 orders of magnitude above typical values reported by others in the literature or ever measured in our own experiments. This implies that the internal resistance is really much closer to the value calculated using Equation (1).

Likewise, the current interrupt method also produces low R_{INT} values unless steady-state conditions are first established. Steady-state conditions and R_{INT} measurements are quickly achieved (within milliseconds) in a conventional fuel cell but take much longer with MFCs, which operate at much lower reaction rates. Unless steady-state conditions have been established (taking up to 30 min), the full picture of the MFC internal resistance losses cannot be produced.

Connecting multiple MFCs in continuous flow requires the units to be fluidically joined to an inflow and an outflow stream. As shown in Figure 3, in order to obtain the maximum power out of the system, the units need to be fluidically isolated, as high shunt losses are incurred due to the 'short-circuit' phenomenon. The stack of 10 fluidically bridged MFCs produced 1250 mV ($\sim 3 \times V_{O\text{-}C}$) instead of the theoretical 4400 V ($10 \times V_{O\text{-}C}$). When the units were isolated, $V_{O\text{-}C}$ (3600 mV), although still 20% lower than the theoretical maximum, was nearly 3-fold higher than that from the fluid-linked stack. Approximately 20% of the voltage lost was due to the instrumentation input impedance (1 MΩ) and a further 5% to instrumentation inaccuracy (0.2%), leaving the remaining 75% that was probably due to the electrical leakage on the outside of the MFCs due to the humid/wet conditions coupled with the

Table I. Comparative data for the small-scale MFC as an individual unit and stacks of 5 and 10 units in parallel, medium-scale MFC as an individual unit and stacks of 5 units in parallel and large-scale MFC as an individual unit under optimum load conditions

MFC conditions	Total anode volume (mL)	$V_{O\text{-}C}$ (mV)	P_{Mean} (μW)	$P_{Density}$ (mW m) ±SD*	$P_{Density}$ (W m^{-3}) ±SD*
1 Small unit	6.25	447	4.7	0.78±0.08	0.75±0.08
5 Small units	31.25	445	31.4	0.930.09	1.00±0.09
10 Small units	62.50	449	60.2	0.890.07	0.97±0.08
1 Medium unit	25	450	12.3	0.450.05	0.49±0.04
5 Medium units	125	448	68.7	0.510.06	0.55±0.05
1 Large unit	500	445	104.4	0.17±0.02	0.21±0.01

*Mean power density per single unit derived from repeated measurements ($n = 3$).

Copyright © 2008 John Wiley & Sons, Ltd.

DOI: 10.1002/er

Table II. Comparative data for the small size MFCs connected consecutively in parallel, under optimum load conditions

Number of MFC units	Total anodic volume (mL)	V_{Mean} (mV)	I_{Mean} (μA)	P_{Mean} (μW)	$P_{Density}$ (mW m^{-2})	$P_{Density}$ (W m^{-3})
1	6.25	64.10	64.23	4.69	0.78	0.75
2	12.50	102.58	102.79	10.81	0.80	0.86
3	18.75	131.05	131.31	17.37	0.86	0.93
4	25.00	159.51	159.83	25.61	0.95	1.02
5	31.25	176.93	177.29	31.41	0.93	1.01
6	37.50	195.18	195.57	38.21	0.94	1.02
7	43.75	211.62	212.05	44.90	0.95	1.03
8	50.00	223.70	224.15	50.18	0.93	1.01
9	56.25	230.47	230.93	53.23	0.88	0.95
10	62.50	245.91	246.40	60.61	0.89	0.97

hygroscopic properties of the plastics/polymers employed in construction.

Electrode potentials can also be affected by pH and, for this reason, during the experiments it was ensured that both the anolyte and the liquid hydrating the cathode were at neutral pH.

Fluidic conductance is less of a problem for a parallel-connected stack, in which the anodes and cathodes are already electrically joined together. However, for a series-connected stack, in which the anodes and cathodes need to remain isolated, fluidic conductance can have detrimental effects (see Figures 4–6). This was found to be more marked when the fluid medium contained higher levels of salt electrolyte (results not presented). The parallel-connected stack offers high amperage but low voltage, whereas the series-connected stack offers high voltage but low amperage. The trade-off between the two appears to be a series/parallel configuration, in which even if there is fluidic conductance, shunt losses are less severe. However, even in this case, as Figure 4 illustrates, P_D can be further increased by 2.5-fold if the units are kept fluidically isolated. This is further strengthened by the data presented in Tables I and II, which show the increase in the mean power output and power density from connecting multiple units together. Data in Table II suggest that the collective power density from stacks of parallel units increases with numbers of units joined together (up to 6–8 units). Further addition of units did not result in any further power density increases. This suggests that for multiple unit networks, there may be an optimum number of cells that can be connected in parallel (i.e. in one configuration), before stacks are joined in series (i.e. in another configuration). Based on power output from 10 small units, a theoretical projection to 80 small units (giving the same equivalent anodic volume of 500 mL as the large unit) gave a projected output of 10 W m^{-3}, which is 48 times higher than the actual output produced by the large MFC.

System efficiency has been described in terms of MPT (see Section 2.7). However, efficiency can also be expressed in terms of the energy output/energy input ratio, which is relevant to the fuel utilization efficiency. The fuel utilization efficiency of the medium-sized MFC for exemplar substrates has already been reported [4]. Although both definitions of efficiency can be used to express the behaviour of MFCs, the former is the most useful for predicting power requirements of real applications and optimising configurations.

With regards to the MFC power output, based on a carbon veil electrode and the limits of scale that we tested, it is clear from our data that scale-up results in a decrease of power per unit volume (or weight). As all sizes of MFC produce the same open-circuit voltage, and power is a function of voltage (V) $\times$ current (I), for MPT conditions, the current (and hence power) is determined by $R_{INT}+R_L$. Therefore, the most likely explanation for loss

Copyright © 2008 John Wiley & Sons, Ltd.

DOI: 10.1002/er

of power upon scale-up is the increase of R_{INT} of the anodic chamber. There are several contributing factors that affect the overall R_{INT} including electrode and electrolyte resistivity and proton path length. Considering the electrode, then R_{INT} depends on the quantity and conductivity of the material as well as its shape and composition. A solid block of a highly conducting anode when scaled up in volume would have a lower resistance as this is directly proportional to the material resistivity (ρ) and material length (λ), but inversely proportional to the material surface area s.a. (A) (i.e. $R = (\rho \times \lambda)/A$). However, a block of anode is inadequate for encouraging microbe–electrode interactions, which require a large s.a. interface. The volume-to-s.a. ratio for a solid block of anode is poor on scale-up as volume (and weight) of the electrode increases to the cubic power of the size measurements (n^3), whereas the s.a. increases only to the square (n^2). In order to improve s.a. for the same unit volume of electrode, the shape or surface must be highly convoluted. For these reasons, carbon fibre veil electrodes are often selected by researchers as a suitable, well-convoluted electrode material providing a high s.a. within a small volume that allows permeation and interpenetration of fluids and fluid transport (mass flow and diffusion) to the microbes. Electrodes made from flat materials (convoluted, mesh or veil) need to be folded into blocks of conducting material and as they increase in amount (size) they tend to increase in resistance with length (whether measured in the weft or the weave directions of the sheet).

A second possible reason for increased R_{INT} on scale-up is in relation to the properties of the fluid electrolyte rather than the electrode; the resistance increases with electrolyte volume. In addition and as previously described, the shorter the distance between the working electrodes and the PEM, the higher the power output [30]. In large anodic chambers, it is more likely that a higher percentage of the microbial activity and proton formation will be taking place 'some distance' away from the interface between microbes and the PEM window and are electrogenically futile (e.g. fermentation) that uses substrate but does not produce electrons. R_{INT} may also be affected by the microbes themselves (which are resistive by nature) and their metabolic products that influence the conductivity of the anolyte.

Another reason largely independent of R_{INT} may also be given for power loss on scale-up relating to mass flow and diffusion. In a small anodic chamber, the fluid transfer through the electrode matrix is not problematic as the matrix is thin layered and highly porous. However, in a much larger electrode system, there are more stagnant regions within the electrode deprived of fuel supply. Diffusion limitation replaces mass flow as a limiting factor for substrate supply and electron production. This effect is observed if a large electrode s.a. is compacted into the anodic chamber, regardless of volume.

Table I is a comparative summary of the long-term steady-state power output from the three different sized MFCs measured as per MFC unit and as multiples of units for the cases of small and medium MFCs only. The data are also expressed as power per m^2 anode electrode area and power per m^3 of anodic chamber volume. In this study, the optimum external resistor value was determined in two stages. Firstly, the cell polarization method was employed, which indicated the external load at which maximum power was produced. Then the three different external resistors, 430 Ω (small), 1.3 kΩ (medium) and 3 kΩ (large), were connected to the respective MFCs to examine the performance under steady-state conditions (see Table I). During these long-term experiments and in the cases where there was no second MFC running under open-circuit conditions (e.g. large MFC), the current interrupt method was employed to measure $V_{O\text{-}C}$. R_{INT} was then recalculated and, if necessary, R_L was readjusted to match the new R_{INT} value. In all cases, the new recalculated value was the same as or close to the original (within 5%).

Table II is a summary of the power output from the process of consecutively connecting multiple small-scale MFCs in parallel. Some of the data also appear in Table I; however, Table II is used to break down the output parameters from the stack configurations, thereby emphasizing and justifying the increase in power density as the number of units increases (up to the optimum point).

Copyright © 2008 John Wiley & Sons, Ltd.

DOI: 10.1002/er

5. CONCLUSIONS

The novelty of this study lies in the demonstration that for a given volume, compartmentalization into as many units as possible, with a concomitant decrease of the individual unit size, results in a more efficient microbial-power harvesting system that could produce higher energy density levels, provided potential power losses from the multiple unit inter-connections are kept at a minimum. This first part of our investigation naturally led to the second aim of this work, which was to study the way that collectives of small units may best be joined electrically to produce useful amounts of power (sufficient to drive small robots).

The term optimal load has been used in the contexts of efficiency, longevity and actual power output, by different groups of workers. For energizing real-world applications it is far more important to deliver maximum power across the load than it is to be highly efficient. Therefore, in this study, the term is used from the perspective of sustainable MPT, which is achieved when the resistive part of the internal impedance is matched by the external resistive load.

The internal resistance, R_{INT}, is a significant parameter of MFCs, as previously identified by numerous workers [11,18,20,23,30]. Equation (1) is a well-established formula in the field of physics and shows a good method of estimating the overall internal losses for impedance matching to achieve maximum power output. Furthermore, it emphasizes the importance of the open-circuit voltage ($V_{\mathrm{O\text{-}C}}$), as an essential parameter for calculating R_{INT}. $V_{\mathrm{O\text{-}C}}$ is an indication of the difference between the standard redox potentials (E_0') of the anolyte and catholyte and defines the force with which electrons will flow through the circuit. As shown in Table I, it is independent of volume and size and, therefore, the same number of units—regardless of size—would be necessary to meet the minimum requirements of the application circuitry. For applications such as mobile robots, this is very important as weight (mass payload) including that of the onboard power supply is a critical constraint that must be kept to a minimum.

With a plurality of small units, series/parallel configurations can be employed to step-up the energy output above the level required to energize real-world electrical or electronic applications. Although this has been previously demonstrated using periodically fed batch culture MFCs, this is the first study to show the advantages of stacks of small-sized MFCs working in continuous flow mode. However, the advantages of further scale-down and plurality have yet to be studied.

ACKNOWLEDGEMENTS

The authors would like to thank the EPSRC for the financial support of this work through the EP/D027403/1 project, Engineering and Physical Sciences Research Council, U.K., database http://gow.epsrc.ac.uk/ViewGrant.aspx?Grant-Ref = EP/D027403/1.

REFERENCES

1. Potter MC. Electrical effects accompanying the decomposition of organic compounds. *Proceedings of the Royal Society London, Series B* 1912; **84**:260–276.
2. Wilkinson S. 'Gastronome'—a pioneering food powered mobile robot. *Proceedings of the International Conference on Robotics and Applications*, Honolulu, Hawaii, 14–16 August 2000, IASTED-2000.
3. Ieropoulos I, Greenman J, Melhuish C. Imitating metabolism: energy autonomy in biologically inspired robotics. *Proceedings of Second International Symposium on Imitation in Animals and Artifacts, SSAISB,* Aberystwyth, Wales, 7–11 April 2003, AISB-03.
4. Melhuish C, Ieropoulos I, Greenman J, Horsfield I. Energetically autonomous robots: food for thought. *Autonomous Robots* 2006; **21**:187–198, DOI: 10.1007/s10514-006-6574-5.
5. Stirling JL, Bennetto HP, Delaney GM, Mason JR, Roller SD, Tanaka K, Thurston, CF. Microbial fuel cells. *Journal of the Biochemical Society Transactions* 1983; **11**:451–453.
6. Bennetto HP, Delaney GM, Mason JR, Roller SD, Stirling JL, Thurston CF. An electrochemical bioreactor for treatment of carbohydrate wastes and effluents. In: *Alternative Energy Sources VII, vol. 4, Bioconversion/Hydrogen*. Hemisphere Publishing Corporation: NY, 1984; 143–157.
7. Bennetto HP, Delaney GM, Mason JR, Roller SD, Stirling JL, Thurston CF. The sucrose fuel cell: efficient biomass conversion using a microbial catalyst. *Biotechnology Letters* 1985; **7**:699–704.
8. Palmore GTR, Whitesides GM. Microbial and enzymatic biofuel cells. In: *Enzymatic Conversion of Biomass for Fuels Production*; Himmel ME, Baker JO, Overend RP (eds). American Chemical Society Symposium, Series, vol. 566, Oxford University Press: Oxford, 1994; 271–290. ISBN13: 9780841229563.

Copyright © 2008 John Wiley & Sons, Ltd.

9. Habermann W, Pommer EH. Biological fuel cells with sulphide storage capacity. *Applied Microbiology and Biotechnology* 1991; **35**:128–133.
10. Gil GC, Chang IS, Kim BH, Kim M, Jang JK, Park HS, Kim HJ. Operational parameters affecting the performance of a mediator-less microbial fuel cell. *Biosensors and Bioelectronics* 2003; **18**:327–334.
11. Park DH, Zeikus JG. Improved cell and electrode designs for producing electricity from microbial degradation. *Biotechnology and Bioengineering* 2003; **81**:348–355.
12. Rabaey K, Lissens G, Siciliano SD, Verstraete W. A microbial fuel cell capable of converting glucose to electricity at high rate and efficiency. *Biotechnology Letters* 2003; **25**:1531–1535.
13. Liu H, Ramnarayanan R, Logan BE. Production of electricity during wastewater treatment using a single chamber microbial fuel cell. *Environmental Science and Technology* 2004; **38**:2281–2285. DOI: 10.1021/es034923g.
14. Logan BE, Cassandro M, Scott K, Gray ND, Head IM. Electricity generation from cysteine in a microbial fuel cell. *Water Research* 2005; **39**:942–952.
15. Ieropoulos IA. *Ph.D. Thesis*, University of the West of England, Bristol, 2006.
16. Bond DR, Lovley DR. Electricity production by geobacter sulfurreducens attached to electrodes. *Applied and Environmental Microbiology* 2003; **69**:1548–1555.
17. Chaudhuri SK, Lovley DR. Electricity generation by direct oxidation of glucose in mediatorless microbial fuel cells. *Nature Biotechnology* 2003; **21**:1229–1232.
18. Jang JK, Pham TH, Chang IS, Kang KH, Moon H, Cho KS, Kim BH. Construction and operation of a novel mediator- and membrane-less microbial fuel cell. *Process Biochemistry* 2003; **39**:1007–1012.
19. He Z, Minteer SD, Angenent LT. Electricity generation from artificial wastewater using an upflow microbial fuel cell. *Environmental Science and Technology* 2005; **39**:5262–5267. DOI: 10.1021/es0502876.
20. Rabaey K, Clauwaert P, Aelterman P, Verstraete W. Tubular microbial fuel cells for efficient electricity generation. *Environmental Science and Technology* 2005; **39**:8077–8082. DOI: 10.1021/es050986i.
21. Cheng S, Liu H, Logan BE. Increased power generation in a continuous flow MFC with advective flow through the porous anode and reduced electrode spacing. *Environmental Science and Technology* 2006; **40**:2426–2432. DOI: 10.1021/es051652w.
22. Delaney GM, Bennetto HP, Mason JR, Roller SD, Stirling JL, Thurston CF. Electron-transfer coupling in microbial fuel cells. 2. Performance of fuel cells containing selected microorganism-mediator-substrate combinations. *Journal of Chemical Technology and Biotechnology* 1984; **34B**:13–27.
23. Oh S, Min B, Logan BE. Cathode performance as a factor in electricity generation in microbial fuel cells. *Environmental Science and Technology* 2004; **38**:4900–4904. DOI: 10.1021/es049422p.
24. Kang KH, Jang JK, Pham TH, Moon H, Chang IS, Kim BH. A microbial fuel cell with improved cathode reaction as a low biochemical oxygen demand sensor. *Biotechnology Letters* 2003; **25**:1357–1361.
25. Zuo Y, Cheng C, Call D, Logan BE. Tubular Membrane Cathodes for Scalable Power Generation in Microbial Fuel Cells. *Environmental Science and Technology* 2007; **41**:3347–3353. DOI: 10.1021/es0627601.
26. Jong BC, Kim BH, Chang IS, Liew PWY, Choo YF, Kang GS. Enrichment, performance and microbial diversity of a thermophilic mediatorless microbial fuel cell. *Environmental Science and Technology* 2006; **40**:6449–6454. DOI: 10.1021/es0613512.
27. Ieropoulos I, Melhuish C, Greenman J. Artificial gills for robots: MFC behaviour in water. *Bioinspiration and Biomimetics* 2007; **2**(3):S83–S93. DOI:10.1088/1748-3182/2/3/S02.
28. Larminie J, Dicks A. *Fuel Cell Systems Explained*. Wiley: Chichester, U.K., 2003.
29. Aelterman P, Rabaey K, Pham TH, Boon N, Verstraete W. Continuous electricity generation at high voltages and currents using stacked microbial fuel cells. *Environmental Science and Technology* 2006; **40**:3388–3394. DOI: 10.1021/es0525511.
30. Liu H, Cheng S, Logan BE. Power generation in fed-batch microbial fuel cells as a function of ionic strength, temperature, and reactor configuration. *Environmental Science and Technology* 2005; **39**:5488–5493. DOI: 10.1021/es050316c.

Copyright © 2008 John Wiley & Sons, Ltd.